«Оптика атмосферы и океана», **27**, № 1 (2014)

ПИСЬМА В РЕДАКЦИЮ. ДИСКУССИОННЫЕ ВОПРОСЫ

Photophoresis and accommodation

H. Rohatschek*

Institut für Experimentalphysik, Johannes-Kepler-Universität, A-4040 Linz (retired)
Lüfteneggerstraße 15, A-4020 Linz, Austria

Поступила в редакцию 1.09.2011 г.

There are two types of photophoretic forces, the ΔT_S- (Crookes) and the $\Delta\alpha$-force (Knudsen). This paper deals with the fundamental problem of distinguishing by experiment between both forces by using their different dependencies on pressure. We explored gravito-photophoresis of individual particles from three materials differing in their physical properties (carbon amorphous, crystalline, aluminium). On the grounds of available aerosol theory representation of the majority of cases is not feasible. Resolvable special cases and the data in their entirety, however, secure unambiguously earlier hypotheses that the force of gravito-photophoresis is normally caused by differences in the accommodation coefficient ($\Delta\alpha$) over the surface. That conclusion is confirmed by a method for determining the size of particles from the force-pressure diagram which yields reasonable results. Hypothetical application of gravito-photophoresis to atmospheric aerosols now obtains empirical corroboration. Some aluminium particles surprisingly show changes in behaviour depending on pressure and irradiance. Here, the levitating force is determined not only (as usual) by the momentary irradiation, but also by the previous history of this factor. We assume that with some metals the irradiation can induce variations in the accommodation coefficient. Results of the investigations are applied to clarifying lasting problems of electro-photophoresis and apparent longitudinal photophoresis.

Ключевые слова: aerosols, vertical transport, photophoresis, radiometer forces, accommodation.

Introduction

Photophoresis is induced by radiometric forces acting on suspended, irradiated particles having all six degrees of freedom [1–4]. In the case of *longitudinal photophoresis*, which can occur with both solids and liquids, the motion takes place in (light-positive) or against (light-negative) the light direction. In the cases of *gravito-*, *electro-*, and *magneto-photophoresis* the field concerned exerts an aligning action on solid particles, whereby an independent body-fixed photophoretic force becomes related to the field. The force can have any angle with the field. The result is generally helical motions around the space-fixed reference direction concerned. *Light-* or *auto-photophoresis* is another type related to the light direction. It differs from longitudinal photophoresis by manifold helical paths. The smaller a particle subject to a body-fixed force, the more these regular motions are superimposed by molecular disturbances. If the directing torque is weak or it vanishes, then *irregular photophoresis* occurs [5].

One has to distinguish between two relevant kinds of radiometric force. First, the Crookes force [6] or ΔT_S-force, which is caused by differences in the surface temperature T_S. Second, the Knudsen force [7] or $\Delta\alpha$-force, caused by differences in the accommodation coefficient α over the surface.

Longitudinal photophoresis is explained by ΔT_S-forces induced by unilateral irradiation [8]. The body-fixed forces acting with field-oriented types of photophoresis are now ascribed in most cases to $\Delta\alpha$-forces. With light-photophoresis both ΔT_S- and $\Delta\alpha$-forces act together.

It may seem to be a matter of course to identify those forces that are rigidly linked to a particle with $\Delta\alpha$-forces, as these are connected to surface properties. Nevertheless, we have to keep in mind ΔT_S-forces, too, since strong linkage or even fixation to the body also occurs with the latter. For the surface temperature, the direction of incident radiation may become less important than the boundary conditions of heat conduction. It is known from macroscopic radiometers made from blank sheet having edges or points that such parts are leading in the motion, independent of the light direction. The cause is that projecting parts remain cooler than the rest of the body. That "point radiometer" effect probably gave rise to gravito-photophoresis observed with millimeter-sized fibrous particles scraped from black paper [9].

Evidently, that fundamental question must be decided by experiment. An opportunity presents itself by the differing pressure dependencies of ΔT_S- and $\Delta\alpha$-forces [10]. We have planned a comprehensive investigation of gravito-photophoresis [11] depending on pressure and irradiance. The experiments described here deal with various particles which move in a horizontal beam of light exactly or approximately in or against the direction of gravity or can be held in suspension. We measured on individual specimens the vertical velocity depending on the irradiance at constant pressure, and, mainly, the irradiance of suspension as

* Hans Rohatschek (hans_rohatschek@yahoo.de).

a function of pressure. From these data the vertical force component has to be inferred.

We have solved our task by the statement that the force acting with gravito-photophoresis is of the accommodation-induced (Δα) type. We draw particular attention to remarkable changes of the force induced by the irradiation, showing an after-effect. We explain those events in an according way by Δα-actions.

Our results permit also answers to problems with other types of photophoresis not understood up to now. We discuss the research about electro-photophoresis depending on irradiance and pressure [12]. The finding by Lustig and Söllner [13] that strongly absorbing silver particles can show negative photophoresis excited vehement disputes because that effect could not be explained by ΔT_S-forces (e.g., [14]). We propose a solution involving both ΔT_S- and Δα-forces (light- or autophotophoresis).

Basic knowledge on photophoresis is important to its applications. To all appearances, gravito-photophoresis is needed for understanding certain phenolmena with aerosols in the middle atmosphere up to the mesopause [15–18]. Krauss and Wurm [19] refer to photophoresis to explain several phenomena in young circumstellar disks forming planetary systems.

Considering our observations of changes of the photophoretic force we should like to encourage experimental research based on Knudsen's radiometric force that may pave the way for novel knowledge on the nature of accommodation.

Preliminaries

For our topic it is essential that ΔT_S- and Δα-forces depend on the pressure in different ways. We will assume that the photophoretic force F can be described by the phenomenological formula

$$F = C\, f(p)\, H(I), \qquad (1)$$

where $f(p)$ comprises the pressure function and no external parameter except the pressure p, H is the net molecular heat flux.

A representation covering the entire range of pressures has been given for spheres [10], see Fig. 1.

In the case of ΔT_S-forces we have

$$CH = \hat{F}, \quad f(p) = \frac{2}{p/\hat{p} + \hat{p}/p}, \qquad (2)$$

where $\hat{F}$ denotes the maximum of F and $\hat{p}$ the pressure where the maximum occurs. For the Δα-force we have

$$CH = F_0, \quad f(p) = \frac{1}{1 + p^2/p^{*2}}. \qquad (3)$$

There, p^* is a characteristic pressure associated to a Knudsen number about 1/2, $\hat{F}$ is proportional to the temperature difference ΔT_S, F_0 to the difference Δα in the accommodation coefficient over the surface.

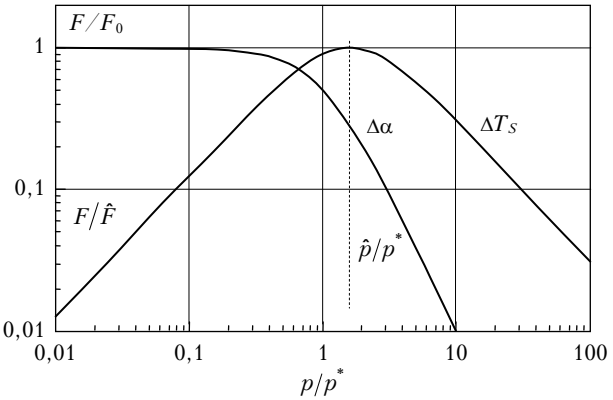

Fig. 1. Scale diagram of both types of photophoretic forces F acting on spheres as function of pressure p, at constant molecular heat flux H. The ΔT_s-force is caused by a temperature difference over the surface, the Δα-force by a difference in the accommodation coefficients

The powder particles used in our experiments were not spherical, but distinctly irregular in shape. At Knudsen numbers about unity, we must be prepared for force-pressure functions deviating from those in equations (2) and (3). On the other hand, the asymptotic behaviour in the limiting cases of very large and very small Knudsen numbers should be well represented by those equations.

Gravito-photophoresis is based on two requirements: a body-fixed photophoretic force and a restoring torque which tends to align the particle with the direction of gravity [20]. That torque originates from a sufficiently large distance between the centre of gravity and the centre of reaction where the resistance force attacks. Under the interaction of photophoretic force and torque, the resistance force and torque, and the gravity-related restoring torque the particle quickly attains a steady state of motion where it rotates around a vertical line and describes a helical path about the line. The body-fixed photophoretic force **F** rotates jointly with the particle. Let the angle between **F** and the direction of gravity $\mathbf{g}/g$ be denoted by ε, then we have

$$F_g = F\cos\varepsilon. \qquad (4)$$

The body-fixed character of the photophoretic force can easily be explained by Δα-forces, as these are connected to surface properties.

Nevertheless, we keep in mind ΔT_S-forces, too, since strong linkage or even fixation to the body is also possible with those. For the surface temperature, the direction of incident radiation may become less important than the boundary conditions of heat conduction. It is known from macroscopic radiometers made from blank sheet having edges or points that such parts are leading in the motion, independent of the light direction. The cause is that projecting parts remain cooler than the rest of the body. That "point radiometer" effect probably gave rise to gravito-photophoresis observed with millimeter-sized fibrous particles scraped from black paper [9].

The sole quantity accessible to direct measurement is the vertical velocity component v_g. From v_g the component F_g of the photophoretic force **F** in the direction of gravity has to be inferred. Our aim is representing the experimental data in a way that the pressure function $f(p)$ in equation (1) becomes transparent.

H satisfies the energy balance

$$AI + E_{abs} = H + E_{emi}, \tag{5}$$

which includes the flux of energy AI absorbed from incident light (A absorption cross section), the energy flux E_{abs} absorbed from the thermal radiation of the surroundings, and the flux E_{emi} emitted by thermal radiation from the particle.

Substituting equation (1) into (4) and using (5) we obtain the formula

$$F_g = Cf(p)AI\left[1 - \frac{E_{emi} - E_{abs}}{AI}\right]\cos\varepsilon. \tag{6}$$

There are two experimental ways to determine F_g depending on I and p in the relation to the weight force mg.

Method A: One measures the vertical velocity v_g at, in each case, fixed pressures and varies the irradiance. Extrapolation to zero irradiance permits determination of the settling velocity v_s in the dark [14]. The force in demand can be found by

$$\frac{F_g}{mg} = \frac{v_g}{v_s}. \tag{7}$$

This procedure would have to be repeated at divers pressures. Here, the presupposition is made that the mobility B is a constant.

Method B: One measures that irradiance $I^{(0)}$ where the particle is exactly held in suspension, that is, where $v_g = 0$, hence

$$F_g^{(0)} + mg = 0. \tag{8}$$

The superscript (0) denotes the condition of suspension. Again, this procedure would have to be reproduced at varying pressures. From a substitution of (6) into (8) we can derive the formula

$$\frac{1}{I^{(0)}} = \frac{C}{mg} f(p) A^{(0)} \left[1 - \frac{E_{emi} - E_{abs}}{AI}\right]^0 (-\cos\varepsilon^{(0)}). \tag{9}$$

A plot of $1/I^{(0)}$ over p is equivalent to one plot of $F^{(0)}/mg$ for I = const according to equation (6), using method A.

It is not difficult to estimate the expression $1 - (E_{emi} - E_{abs})/AI = H/AI$ [10]. For pressures exceeding typically 1 hPa, the net energy flux emitted by thermal radiation, $E_{emi} - E_{abs}$, can be neglected because of the moderate temperature elevation. This implies that practically all energy absorbed from the incident light, AI, is re-emitted by molecular transfer, H. As the pressure decreases below that order, the particle becomes significantly hotter, and H/AI declines below unity.

The absorption cross section A can vary if the position of a nonspherical particle to the incident light beam changes, furthermore because of variations of the wavelength spectrum with the lamp temperature (Table 1).

Table 1

Relation between the lamp voltage $U_L(V)$, the irradiance (W/m^2) without filter, I_0 with infrared absorbing filter, I_{IR} and the ratio I_{IR}/I_0

U_L	9	10	11	12	13	14	15	16
I_0	1940	2380	2830	3290	3780	4260	4790	5320
I_{IR}	133	190	259	336	430	546	673	805
I_{IR}/I_0	0.069	0.080	0.092	0.102	0.114	0.128	0.141	0.151

In contrast to these two minor effects, a change in the position can produce consequences in quality to cosε. That factor can vary between the limits +1 (down) and −1 (up). More than the other factors in equation (6), cos ε will influence the results. Covering that subject would claim for complete knowledge of the mechanics.

The objects of this study differ from those usually investigated in double regard: they are irregularly shaped and possess masses so large as inertial reactions can no longer be neglected compared to the other forces. Doubtless, rotational inertia (characterized by the rate of change of angular momentum) appears with photophoresis for the first occasion in aerosol physics.

General equations of motion for photophoresis have been given by [21, Eq. (36)]. Solving these equations may become enormously complicated and must be limited to special cases. In that paper the case of a nonspherical body, yet without inertia, is realized. There exists one single publication on photophoresis where rotational inertia has been taken into account, demanding solution of Euler's equations [22].

However, the theory is obstructed on the whole because calculation of the resistance forces on arbitrary particles, needed for the entire range of Knudsen numbers, is possible only for the limiting cases of very low [23] and very high [24] Knudsen numbers.

The ideal aim of assembling a supply of computations of solvable uses, whereby many physical parameters are varied on a wide scale, can not be attained at the present state of affairs. Therefore, excepting special cases, statements on cos ε were not possible. The lines inscribed in the figures are fitting curves to the experimental data.

Experimental equipment

The investigations of the dependence of gravitophotophoresis on the pressure and the irradiance are carried out on aerosol particles suspended in an evacuated chamber which a horizontal light beam traverses. That beam is produced by an optical system similar to a projector. This ensures that in the observation section, situated in the middle of the chamber, the irradiance is fairly homogeneous. The cross section of the beam, there, forms a square of 20×20 mm. The light

source is a halide lamp 24 V/250 W, the irradiance can by adjusted by the supply voltage. Our interest is concentrated on particles which ascend more or less vertically within the beam and remain suspended at its upper edge.

That apparatus has previously been described in detail [15, 25]. Some slight modifications have been realized. For the aim of observing individual particles at varied pressures, an electrostatic device for holding a particle during the change of pressure (but not during observation) has been added to the arrangement shown in [15, Fig. 1]. One electrode is formed by the sample reservoir, consisting of a cylindrical metal tube whose bottom is a grid. The other electrode is a surrounding concentric metal ring positioned in the plane of that bottom. This plane has a distance of several millimeters to the upper edge of the beam. The reservoir is connected to the grounded wall of the chamber, the ring to a positive or negative constant voltage up to 50 V.

The beam-bounding pupil, a rectangular opening, is held constant during each series of measurements. In order to work at low irradiance without loss of visual brightness, an infrared absorbing filter can be inserted. Both the variation of the radiation temperature and the elimination of a substantial infrared fraction cause changes in the energy spectrum, see Table 1. Depending on particle substance and size, this may have consequences to be taken care of. We have put up with these disadvantages in view of the advantages of continuous and reproducible variation of irradiance over a wide range.

Immediately after a series of measurements the irradiance corresponding to each lamp voltage set can be determined by means of a thermopile. Thereby, the chamber is removed. Losses in one glass window and, in that case, in the IR-filter are taken into account. The pressure is measured by an instrument combining a compression vacuum-gauge with a U-tube.

The particles are observed through a 6× magnifying microscope perpendicular to the directions of light and gravity. For locating a particle or determining its vertical velocity component, the microscope is equipped with horizontal lines on the ocular frame.

Experimental procedure

The samples used were a powder made from charred sunflower marrow (CSM) and commercially available powders of graphite (C) and aluminium (Al), all of the size orders 1 and 10 μm. Electron micrographs of the latter have been shown in [15].

The standard procedure starts with releasing a swarm of particles from the reservoir by knocking on the cover of the chamber. Some of the particles remain in equilibrium at the upper edge of the light beam. A suitable particle is selected by making it repeatedly descend and rise, normally by operating the IR-filter.

The usable pressure interval extends from about 0.5 to about 50 hPa. Below the order of 1 hPa the mobility becomes excessively high, and suspended particles tend to escape at the slightest perturbation. Above the order of 10 hPa convection currents can impair the observations. Those currents originate from heating of the entrance and exit windows at the transmission places of the light beam.

While the pressure is changed, the particle is held at the upper edge of the beam, near the axis of the radially symmetric auxiliary electric field. This field is also used to centre a particle before each observation. During any measurement on gravito-photophoresis that electric field must remain switched off, because it might exert a directing action on the particle, and thus falsify the effect of interest by producing electro-photophoresis.

For experimentally finding the dependence of F_g on the pressure, we used both methods mentioned in the introduction. Method A requires measuring v_g as a function of I at a series of values of p. For each pressure, the object must be lifted several times over a vertical distance of more than 5 mm. Thereby particles soon got lost, in particular at low pressures. So F_g, could not be measured at all planned values of p and I.

With method B, the particle is observed in or about the state of zero vertical velocity. This circumstance involves many advantages for the practical execution. We succeeded in performing such measurements with more than 100 particles. If a particle is found which ascends at average irradiance, then its magnitude is carefully adjusted such as the particle remains suspended at a definite height a small distance below the upper edge of the beam. Thereby it stays within that part of the cross section where the distribution of irradiance is practically homogeneous.

A series of measurements normally starts near the low or also the high end of the available pressure range. The pressure is then varied in approximately equal steps indicated on the logarithmic scale of an auxiliary thermal conductivity gauge.

Let us start from a state of suspension. There, Eq. (8) is satisfied. If the pressure is decreased or increased, a limit can be attained where the particles can no longer be held in suspension and the particle drops out. Sometimes this is due to not sufficient irradiance, but mainly it is the factor $-\cos\varepsilon$, which can become negative and then Eqs. (12), (13) are unsolvable.

Another type of restriction is the non-ideal behaviour of a particle. In an ideal case of gravito-photophoresis the motion follows an exactly vertical path. In the state of suspension that particle rotates on a narrow circular orbit without lateral shift. However, even if a particle has been selected at a certain pressure for sake of its strictly vertical motion, at higher pressures it happens that a motion in or against the direction of light adds to the vertical motion. If that particle is brought to suspension, it will drift along the beam. Up to some extent, the determination of zero vertical velocity nevertheless remains well-defined and meaningful. But finally, if that particle before the measurement is released from holding by the auxiliary electric field, it can quickly drift away.

These effects can be explained by ΔT_S-forces in the form of a motive force or a directional torque related to the direction of light [25].

Results

Our attempts to realize method A yielded as a by-product some functions of v_g depending on I at fixed pressures. Examples of particles from carbonized sunflower marrow are shown in Fig. 2. (The notation "Pk" for the particle number means "Probekörper".) These particles exhibit linear plots, at least initially. Hence it follows that the original restoring torque is still dominating the total driving torque. Such characteristic not necessarily continues with increasing irradiance, since previous investigations furnish evidence that even a transition from ascending to sinking movement can occur [15, e.g. particle No. 148]. The plot of Pk 5 is linear at the beginning and tends finally to bend towards lower values. A behaviour like this may be caused either by a change of cosε while the axis of rotation remains vertical, or in some cases by a deviation of that axis from the vertical direction due to an increasing influence of ΔT_S-forces. Since the protocol for Pk 5 notes a growing deviation from vertical movement, the latter cause is more probable in that particular case.

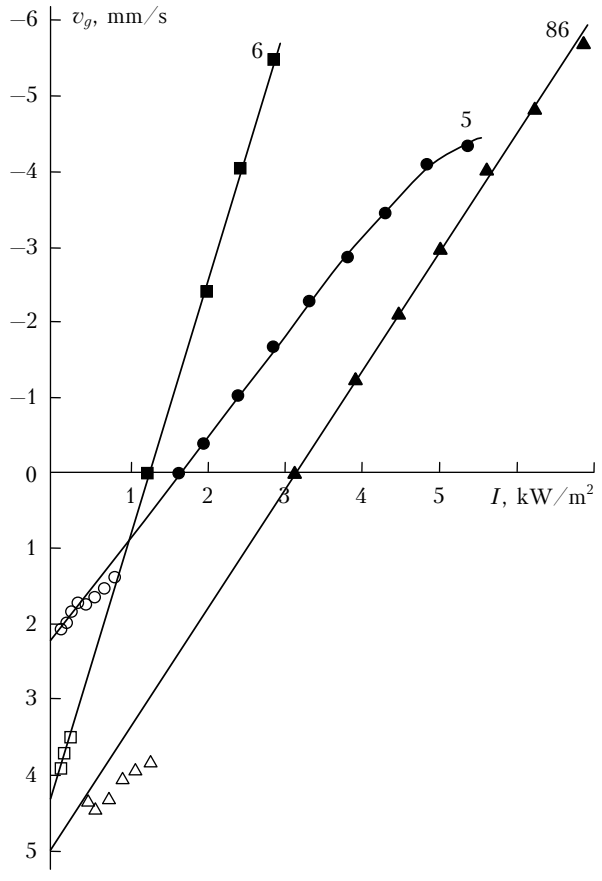

Fig. 2. Vertical velocity component v_g as a function of the irradiance I. Full data signs: measurements without, empty sign: wit h infrared absorbing filter. Particles of carbonized sunflower marrow. Pk 5: p = 8.5 hPa, v_s = 2.2 mm/s, $I^{(0)}$ = = 1.6 kW/m^2, Pk 6: p = 3.5 hPa, v_s = 4.4 mm/s, $I^{(0)}$ = = 1.25 kW/m^2: Pk 86: p = 3.6 hPa, v_s = 5.0 mm/s, $I^{(0)}$ = = 3.1 kW/m^2

The measurements with an infrared-absorbing filter proved to be useful for determining the settling velocity v_s by extrapolating v_g to $I = 0$ at low irradiances, but they also raised some problems. With Pk 6, these measurements fit well into the line interpolating those without filter. With Pk 5 and Pk 86 it attracts notice that the measurements with filter group along lines having slopes smaller than the interpolation lines for the measurements without filter: for Pk 5 a slope smaller by a factor between 0.8 and 1, and for Pk 86, by a factor about 0.6.

These observations can be explained by a dependence of the absorption cross section A on the wavelengths which are in the order of the particle sizes. That is, A can decrease if the long wavelengths of the *IR* are removed from the full spectrum. The particle Pk 60 (also CSM, Fig. 4, *b*), a tiny one near the limit of visibility, yielded a ratio of slopes as low as 0.45. This can be inferred from the suspension irradiances $I^{(0)}$ = 0.65 kW/m^2 without and 1.45 with IR-filter. There the pressure was 34.7 hPa.

Fig. 3 to Fig. 7 show the data we obtained using method B. Except Fig. 6, these are presented in logarithmic diagrams conforming to Eq. (13). The reciprocal suspension irradiance $1/I^{(0)}$ is plotted as a function of the pressure p.

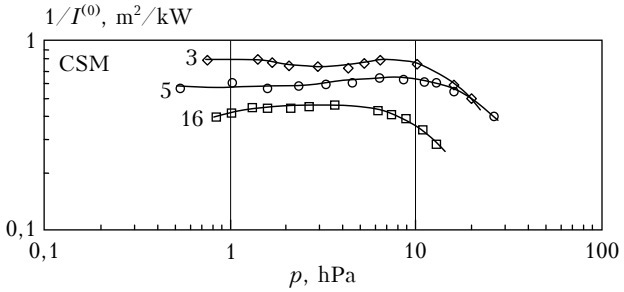

Fig. 3. Reciprocal suspension irradiance $1/I^{(0)}$ depending on the pressure p, carbonized sunflower marrow. Selection of graphs showing a wide plateau. Sequence of measurements from low to high pressures

The ratios of maximum to minimum pressure for measurements on individual particles extend from about 20 to 25 (for a group including Pk 6, 64, 101 of CSM, Pk 43, 48 of C and Pk 74, 76, 77 of Al) up to the top values of that ratio, 32 for Pk 94, 50 for Pk 5 and 63 for Pk 97 (shown in Fig. 7).

The lowest values of the suspension irradiance, $I^{(0)} < 1$ kW/m^2, were observed with the following particles (all CSM): Pk 60, $I^{(0)}$ = 0.650 kW/m^2 (Fig. 4, *b*); Pk 95, $I^{(0)}$ = 0.805 kW/m^2 (Fig. 4, *b*); Pk 97, $I^{(0)}$ = = 0.828 kW/m^2 (Fig. 7); Pk 101, $I^{(0)}$ = 0.983 kW/m^2 (Fig. 4, *a*). For some more particles we found values below the solar constant, $I^{(0)} \leq 1.368 = 1/0.731$ kW/m^2: Pk 6, 58, 64 of CSM (Fig. 4, *a*, *b*) and Pk 48 of C (Fig. 4, *c*). Aluminium needs the highest irradiances for suspension: The minimum (Pk 76, Fig. 5, *b*) is $I^{(0)}$ = 2.30 kW/m^2. The maximum values, about 10 = = 1/0.1 kW/m^2 are limited by the admissible lamp voltage.

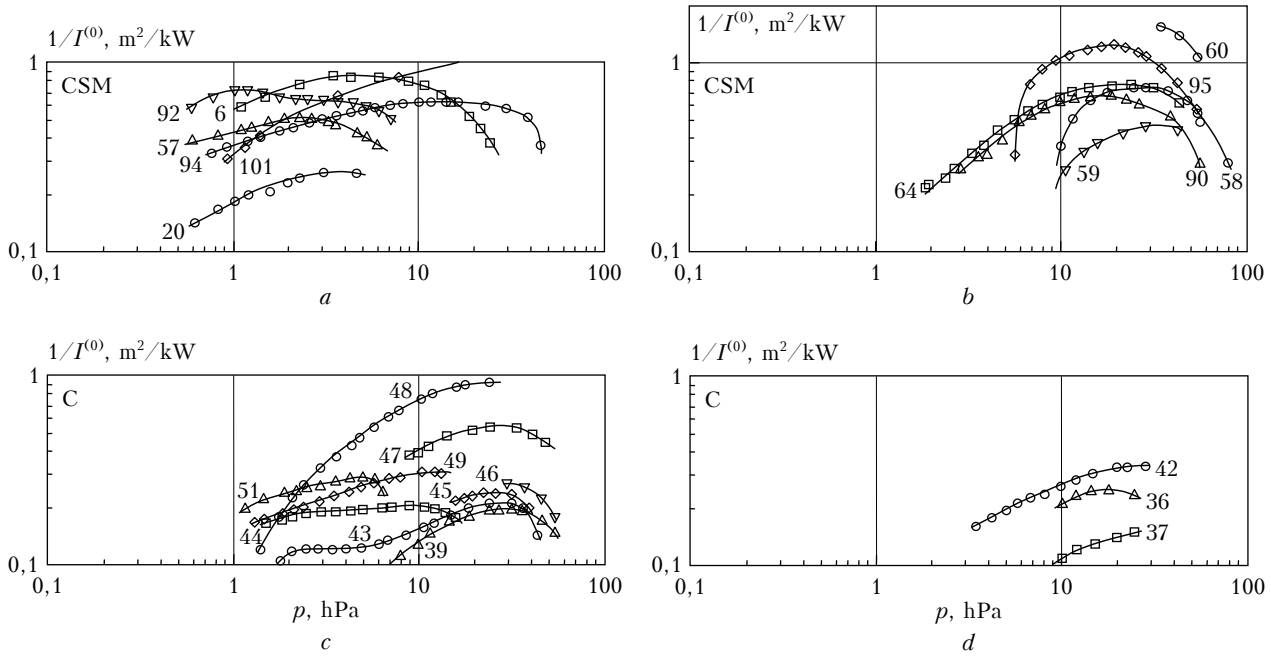

Fig. 4. $1/I^{(0)}$ vs. p. Carbonized sunflower marrow. Sequence from low to high pressures (*a*). Sequence from high to low pressures (*b*). Graphite. Sequence from low to high pressures (*c*). Sequence from high to low pressures (*d*)

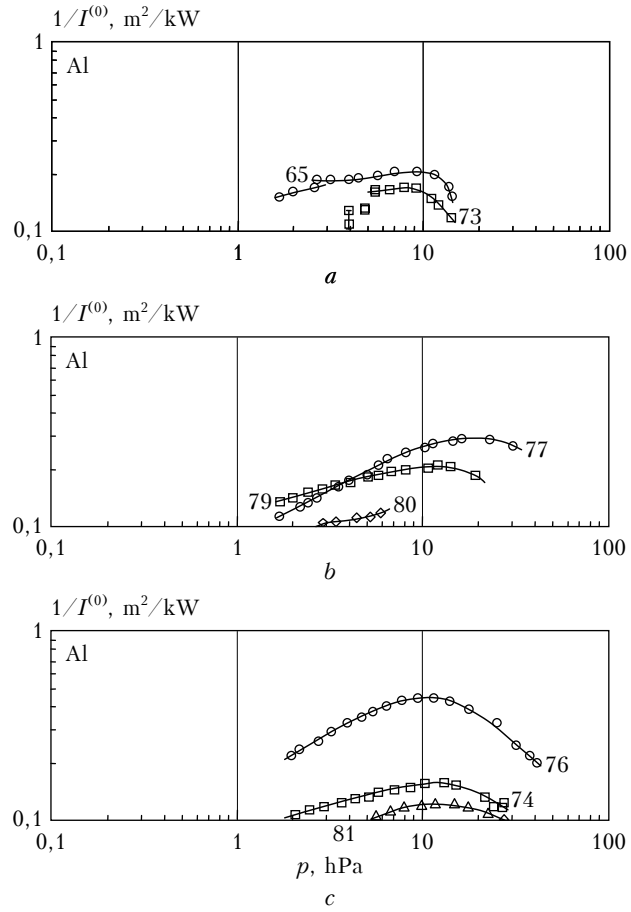

Fig. 5. $1/I^{(0)}$ vs. p. Aluminum. Sequence from low to high pressures (*a*). Sequence from high to low pressures (*b*). Selection of particles showing irregular behavior (*c*)

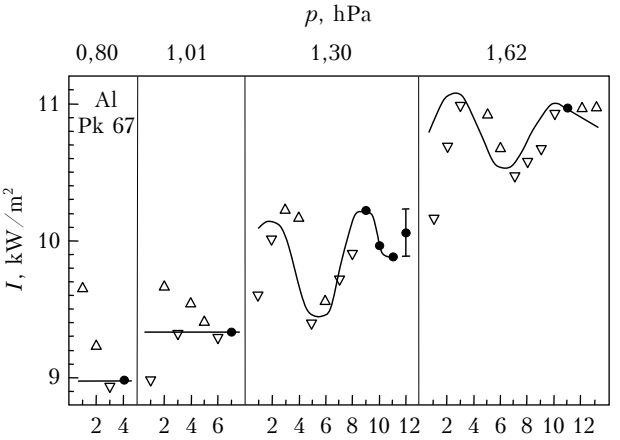

Fig. 6. Aluminum, Pk 67. Irradiance set and sense of vertical motion for consecuting observations (number indicated). Triangle pointing upwards: ascending, triangle pointing downwards: descending, full circle: suspension (at least temporary)

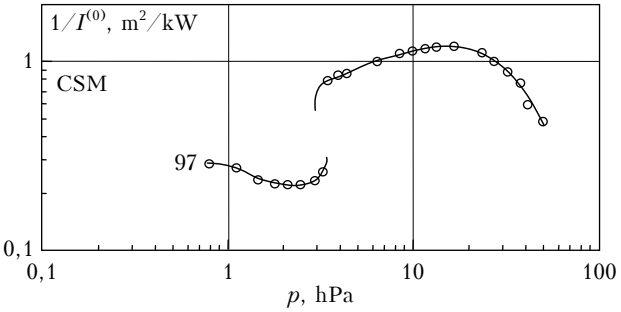

Fig. 7. $1/I^{(0)}$ vs. p. Carbonized sunflower marrow, Pk 97. Graph showing a discontinuity ("catastrophe")

Above all, our aim is inferring from the measurements of $I^{(0)}$ and p the main factor f on the basis of equation (13). In the introduction we have described the distinguished situation where the position of the particle to the direction of gravity practically would not change, that is $\cos\varepsilon \approx$ const. If this occurs, then the pressure function $f(p)$ would come forward.

In Fig. 3 we have compiled some particles of CSM (Pk 3, 5, 16) where obviously such favourable conditions concur. Pk 44 of C (Fig. 4, *c*) is another example. A characteristic common to these graphs is a wide plateau over one decade of pressures or more. At the high-pressure end the transition to a decline can be noticed. These plots fit well with the theoretical curve for $\Delta\alpha$-forces in Fig. 1.

The majority of the particles does not show this special behaviour. Nevertheless, by low variations of $1/I^{(0)}$ over wide pressure ranges, many particles show some degree of similarity with those of Fig. 3. Examples are Pk 6, 57, 92, 94 (Fig. 4, *a*); Pk 64, 90 (Fig. 4, *b*); Pk 43, 47, 49 (Fig. 4, *c*); Pk 42 (Fig. 4, *d*); Pk 77, 79 (Fig. 5, *a*); Pk 74, 81 (Fig. 5, *b*).

If a varying factor $\cos\varepsilon$ is taken into account, then it still appears plausible to interpret this variety of plots by assuming f-functions of the $\Delta\alpha$-type. Even a case like Pk 48 (Fig. 4, *c*) does not oblige to consider ΔT_S-forces. Transitions between plots neighbouring in form can be understood by moderate steps in the physical parameters.

Apparently, even in these general cases there are domains where $f(p)$ comes forward. With several plots extending sufficiently far to high pressures a decline commensurate to that appearing above p^* in Fig. 1 ($\Delta\alpha$) can be noticed. From this, the specific value of p^* can be obtained. There is a relationship between p^* and the radius a of an equivalent sphere. For laboratory conditions it has the form $p^* a = 138$ hPa · μm [10, p. 726]. Applying this method we obtained the data shown in Table 2. Particles marked by "P" were noted in the protocol by "punctuate" or "very small", in agreement with the inferred radii.

Table 2

Material; Pk particle number, p^* characteristic pressure, a radius of an equivalent sphere. "*P*" denotes particles that appeared "punctuate"

Material	Pk	p^*, hPa	a, μm
CSM	3	20	6.9
	5	28	4.9
	6	19	7.3
	16	13	10.6
	57	8.2	16.8
	58	45	3.1 P
	60	51	2.7 P
	95	37	3.7 P
	97	32	4.3 P
Al	76	33	4.2 P

One has to discriminate between these sloping sections of plots fitting in the function $f(p)$, and those which slope away suddenly. Examples are Pk 94 (Fig. 4, *a*) and Pk 43 and 51 (Fig. 4, c). There are also cases of rapid sloping away at decreasing pressure: Pk 58 (7.9 hPa), 59 (8.9 hPa) and 95 (5.6 hPa). Here, the pressures in parentheses indicate limits of possible suspension. Obviously, with these "precipitations" it is the factor $\cos\varepsilon$ which approximates to a value where F_g can no longer balance the weight.

Between the materials there are no differences greater than those within one kind. In regular cases, which are in majority, the measured data remain constant and are reproducible.

With aluminium, however, a surprising phenomenon of variability was found. Fig. 5, *a* and 5, *b* show normal cases, Pk 81 gives an example: The measurements started at 9.8 hPa, continued at increasing pressure up to 31.0 hPa, then the initial pressure 9.9 hPa was set again. The values for $I^{(0)}$ are coincident, and the subsequent measurements down to 4.8 hPa continue the curve.

Fig. 5, *c* shows different occurrences. With Pk 65 the measurements went from 2.7 to 14.1 hPa, where the order was reversed. Although one measurement at 13.4 hPa still fits the curve of increase, the value of $I^{(0)}$ at the initial pressure (2.6 hPa) differs from the first one, and the continuation towards lower pressures deviates from the initial section.

Pk 73 (Fig. 5, *c*) shows more anomalies. The first measurements took place at the pressures 10.9, 11.9, 13.9, 9.1, 7.8, and 6.6 hPa. That far nothing conspicuous happened. The graph is a continuous curve. At the transition from 6.6 to 5.4 hPa the protocol records: "The behaviour has changed somehow". From this pressure downwards the data points in the plot no longer mean enduring suspension irradiances $I^{(0)}$. Rather, at the pressures 5.4 and 4.8 hPa just passing suspensions are indicated. Finally, at 3.9 hPa there was no suspension at all. Initially (lower square, $I = 9.09 = 1/0.110$ kW/m^2) the particle sunk, after enhancing up to $I = 9.74 = 1/0.103$ kW/m^2 the particle rose and carried on rising, while I was decresed (indicated by a bar) to the initial value $I = 1/0.111$ kW/m^2 and finally, at the end of the measurements (upper square) to $I = 1/0.128$ kW/m^2. The particle, a platelet, exhibited perfect gravito-photophoresis by exactly vertical motion and axis of rotation.

These puzzling observations may become more transparent by a representation of the behaviour in the course of time of an Al-particle submitted to changing irradiance (Pk 67, Fig. 6). The abscissa is the number of measurement, the ordinate the respective irradiance set. The abscissa can be read as a qualitative time-axis, since the period between consecutive measurements amounts to rather uniformly about one minute. (Example: the measurements Nos. 11–13 at $p = 1.62$ hPa were timed 0, 76, 120 s.) In the data points the vertical motion is indicated: Triangle vertex up for ascending, triangle vertex down for descending, full circle for suspension (lasting or passing).

At the pressures 0.80 and 1.01 hPa the standard procedure for finding the suspension irradiance works well: if the particle is descending, then I is enhanced, if its is ascending, I is decreased, until suspension is obtained. At the pressure 1.30 hPa a quite different

situation comes to light. During the search for suspension (Nos. 1–3) ascending motion was obtained. At No. 4 it is noted in the protocol: "It looks like something has changed during this pressure setting: decrease of the suspension irradiance". After lowering (No. 5), now the irradiance had to be enhanced (Nos. 6–9). Certainly, states of suspension were obtained (No. 9), but merely passing and varying on between the values of Nos. 9 and 11.

The situation at $p = 1.62$ hPa is like before. The suspension (No. 11) is as well but temporary. The irradiance of No. 11 remains fixed at Nos. 12 and 13, and happens to equal that of No. 3: at the very same irradiance descending, suspension and ascending of the particle occur.

In the irradiance versus "time" plots for the pressures 0.80 and 1.01 hPa, the data points where ascending and descending takes place, can be separated by a horizontal line $I = I^{(0)}$ which intersects the point of suspension. $I^{(0)}$ is constant and depends on the instantaneous irradiance only. We will term states like these, which lead to persistent suspension, "regular".

The cases of the pressures 1.30 and 1.62 represent what we will term "irregular". In order to separate the points indicating ascending or descending twisted curves are required. Possible solutions are inscribed. The vertical force $F_g + mg$ obviously depends not only on the instantaneous magnitude, but also on the previous history of the irradiation. There, a characteristic time of the order one minute enters. The behaviour of the particle and the actions of the observer and operator form a feedback loop which renders periodic processes possible. A period of seven to eight intervals ("minutes") seems to come forward.

The strange behaviour in time at varying irradiance compels us into the conclusion that it is the magnitude of the force F itself and not its orientation ($\cos\varepsilon$) that plays the decisive role, equation (5). We believe that in certain pressure domains the irradiance can influence the accommodation of molecules. The physical cause may be processes in the oxide layer of the aluminium depending on the density of the air and the temperature of the particle.

If we specialize equation (8) to $\Delta\alpha$-forces, we obtain $F = K(\Delta\alpha/\bar{\alpha})f(p)H$, where K is a constant dependent only on properties of the gas. With the irregular states, suspension — equation (12) — is not an unambiguous condition for $I^{(0)}$. By substituting that expression for F into equation (13), where we suppose that A and $\cos\varepsilon$ do not change and $H = AI$, we can derive the condition $(\Delta\alpha/\bar{\alpha})I^{(0)} = \text{const}$. Thus, any change in the suspension irradiance is connected with a change in the difference of accommodation coefficients.

If one and the same particle can be held in suspension at both a higher (h) and a lower (l) irradiance, then the relationship $I_h^{(0)}(\Delta\alpha/\bar{\alpha})_h = I_l^{(0)}(\Delta\alpha/\bar{\alpha})$, must be satisfied.

Example a: Pk 67 (Fig. 6), $p = 1.30$, Nos. 9 and 11. $I_h^{(0)} = 10.23$ kW/m^2, $I_l^{(0)} = 9.90$ kW/m^2; $I_h^{(0)}/I_l^{(0)} = (\Delta\alpha/\bar{\alpha})_l/(\Delta\alpha/\bar{\alpha})_h = 1.033$; relative change in $\Delta\alpha/\bar{\alpha}$ 0.033 (3.3%). In both cases suspension was actually observed.

Example b: again Pk 67, $p = 1.30$. If we admit a virtual state of suspension between Nos. 5 and 6 (9.40 and 9.56 kW/m^2) for the low value of $I^{(0)}$, and take for the high value No. 9. As before, then we obtain: $I_h^{(0)} = 10.23$ kW/m^2, $I_l^{(0)} = 9.48$ kW/m^2; $I_h^{(0)}/I_l^{(0)} = (\Delta\alpha/\bar{\alpha})_l/(\Delta\alpha/\bar{\alpha})_h = 1.079$; relative change in $\Delta\alpha/\bar{\alpha}$ 0.079 (7.9%).

Example c: Pk 73 (Fig. 5, *c*), $p = 3.9$ hPa. Both spots (squares) do not indicate suspension, yet boundaries beyond of which suspension states can be expected. We assume $I_h^{(0)} > 9.20$ kW/m^2 (bottom square), $I_l^{(0)} > 7.94$ kW/m^2 (top square), and find $I_h^{(0)}/I_l^{(0)} = (\Delta\alpha/\bar{\alpha})_l/(\Delta\alpha/\bar{\alpha})_h > 1.159$; relative change in $\Delta\alpha/\bar{\alpha} > 0.159$ (15.9%).

Resuming these examples, relative changes in $\Delta\alpha/\bar{\alpha}$ are in the order of 10%. If we assume a typical magnitude of $\Delta\alpha/\bar{\alpha} = 0.2$ (e.g., $\bar{\alpha} = 0.8$, $\Delta\alpha = 0.16$) then typical changes will amount to 0.02.

The following particle, Pk 97 of carbonized sunflower marrow (Fig. 7), is remarkable by its striking discontinuity. The visual impression was noticed as "punctuate" (see Table 2). The measurements took place at increasing pressures. Between $p = 2.94$ and 3.45 hPa an unusual jump from $I^{(0)} = 4.25 = 1/0.235$ kW/m^2 to $I^{(0)} = 1.28 = 1/0.789$ kW/m^2 occurred. Then, again a lower pressure, $p = 3.24$ hPa, was set, whereat $I^{(0)}$ returned to the higher level $I^{(0)} = 3.82 = 1/0.262$ kW/m^2. At setting $p = 3.39$ hPa, $I^{(0)}$ jumped again to the lower level $I^{(0)} = 1.27 = 1/0.788$ kW/m^2. As the pressure was raised to the final value, $I^{(0)}$ varied continuously whereby very low values below 1 kW/m^2 were reached.

We trace these events back to variations of $\cos\varepsilon$. The processes around the jump will be treated within the frame of catastrophe theory as "fold catastrophe". The branch before the discontinuity is interpolated by a curve which ends with a perpendicular tangent at 3.37 hPa = p_{I}. At higher pressures only a separated branch of the $1/I^{(0)}$-p-graph exists. That second branch, extrapolated towards lower pressures, would not stop at p_{I}. Theoretically, stable states would persist down to an estimated value of about 3 hPa = p_{II}. There the curve, bending downwards, would also end with a perpendicular tangent. (From this point an S-shaped curve, joining p_{II} with p_{I}, formed by unstable states, would complete both branches to a single graph). In the pressure interval between p_{II} and p_{I} two stable states with different $\cos\varepsilon$ would exist. This precondition would have been met at $p = 3.24$ hPa. Suspension was realized in one case for the first branch. Unfortunately, we missed the opportunity of detecting another state of suspension on the second branch at the same pressure. The continuation of the second branch below $p = 3.39$ hPa was not realized by experiment and is, therefore, hypothetical.

Discussion and conclusion

In this chapter we will set principal results of the present investigation in connection with general

questions of photophoresis, and will apply them to clarifying lasting problems with the pressure dependence of electro-photophoresis and apparent longitudinal photophoresis.

It has been supposed years ago [2] that the body-fixed photophoretic forces, postulated for explaining non-longitudinal types of motions, are due to differences of the accommodation coefficients over the surface. The main arguments are these [25]: $\Delta\alpha$-forces are by nature body-fixed. Light-negative motions of large, strongly absorbing particles and the magnitude of the force in cases where ΔT_S-forces must be ruled out, can be understood on that foundation. With the results on the pressure dependence of the force of gravito-photophoresis presented here the $\Delta\alpha$-theory can be considered as well established.

The specimen shown in Fig. 7 with its conspicuous "jump" in the graph is important not only as a curiosity but also because of the mathematical structure it shares with a class of frequently observed photophoretic motions where particles reciprocate on helical paths over a slope in irradiance. (There the pressure is constant). Amongst others those occur with gravito-photophoresis. Such a reciprocation or oscillation can be represented by a plot of the axial force component versus the irradiance having "catastrophic" character like Fig. 7. The plot shows two partly overlapping branches corresponding to opposite axial motions. Reciprocation takes place over that irradiance interval where both branches coexist.

A theoretical model of particles executing helical reciprocations along the direction of a magnetic field was given in [22]. There, an essential element is the inclusion of rotational inertia. We conclude that the case of Fig. 7 has an analogous base.

Electro-photophoresis is a type of photophoresis where particles move in or against the direction of an electric field, even if they are not charged. The regular effect requires a body-fixed photophoretic force and a permanent electric moment. An additional induced moment can modify the phenomena.

Wilflinger investigated the dependence of electro-photophoresis on the light irradiance and the gas pressure [12]. She used tellurium particles of the size order 0.1 μm suspended in nitrogen at pressures between about 120 and 1000 hPa. The procedure corresponded to method A quoted above. The plots of the quotient of the electro-photophoretic force and the weight force versus the pressure show maxima between 400 and 550 hPa or flat regions towards the atmospheric pressure. The curves differ from the ΔT_S-case in Fig. 1. Moreover, in a diagram analogous to Fig. 1 even the plots which have a maximum can not be reduced to a single curve at all. With two particles the pressure dependence of both electro- and longitudinal photophoresis was measured. The maxima of both effects occurred at different pressures.

Wilflinger's results can easily be explained by the hypothesis that the force of electro-photophoresis is a $\Delta\alpha$-force, whereas longitudinal photophoresis is due to ΔT-forces. The plots of her paper resemble our plots of Pk 6, 57, 64, 90, 95; 39, 42, 47; 76, 77, 79 in Fig. 4, *a*–5, *b*. Hence, variation of $\cos\varepsilon_E$ can inferred. It should be noticed that the helical paths of field-oriented types of photophoresis were not yet known. The force of electro-photophoresis was assumed to coincide with the direction of the electric field. Actually, it can have any angle ε_E with the latter, and merely the projection on the field is observed.

As to the analogous effect of magneto-photophoresis, little work was devoted to the pressure dependence. Tauzin [26] described collective phenomena when a stream of iron particles dropped into a magnetic field under simultaneous illumination. Unfortunately no investigations on individual particles at varying pressures have appeared in the literature.

The $\Delta\alpha$-forces are important not only for the explanation of field-oriented types of photophoresis, but also for a class related to the direction of incident light itself (light- or auto-photophoresis). That effect differs by helical paths from longitudinal photophoresis. The standard theory of the latter has been based exclusively on ΔT_S-forces.

Lustig and Söllner [13] published a fundamental investigation of photophoresis of silver-particles in the size order of 0.1 μm, produced by arc discharge and suspended in nitrogen. Settling and photophoretic velocity were measured on individual particles at pressures varied between about 1000 and 100 hPa. A special evaluation of the settling (Kármán's criterion) showed that the particles were uniform in their mechanical properties. Nevertheless, their photophoretic behaviour turned out to be quite different. Besides the majority of light-positive particles, also light-negative ones occurred. With most of them, photophoresis changed essentially in the course of the pressure variation, in dependence on the grade and time of irradiation. A part of the light-negative particles gradually turned to positive photophoresis.

For the standard theory, negative photophoresis of strongly light-absorbing particles created a notoriously intricate problem, as the required higher heating at the back surface could not be explained. A recent treatise incorporating surface-modes neither yielded a solution [14]. Instead, these authors proposed that the Ag-particles seen to move backwards in the L & S paper were clusters. However, this assumption conflicts with the fact that the particles satisfied Kármán's criterion.

We reason that the light-negative motion was "pseudo-longitudinal" photophoresis which can not be explained by ΔT_S-forces alone and claims for incorporation of $\Delta\alpha$-forces. A superposition of both types of forces, combined with a restoring torque related to the direction of incident light, can produce a helical motion, according to circumstances, as well light-positive as-negative auto-photophoresis. Because of the smallness of the particles the helical fine-structure, dominated by Brownian disturbances, could not be detected at those times.

The generation of torques aligning particles to the light direction has been shown for nonspherical bodies acted on by ΔT_S-forces [21]. We suppose that

the variation of $\Delta\alpha$-forces depending on the absorption cross section which varies with the position to the light can produce an analogous directing effect.

Besides the light-negative Ag particles, paper [12] involves another difficult problem, that is, the variation of photophoresis with the pressure and the time and grade of irradiation. We stress the remarkable similarity to the irregular Al-particles described before (Fig. 5, *c* and 6). Both are metals. (The particles were suspended in different gases: Al in air, Ag in nitrogen). We assume that the actual and previous states of pressure and irradiance can induce processes in the surface layers having consequences for the accommodation of the gas molecules.

1. *Preining O.* Die Erscheinungen der Photophorese // Staub. 1955. V. 39. P. 45–64.
2. *Rohatschek H.* Theorie der Photophorese – Ergebnisse und Probleme // Staub. 1955. V. 42. P. 607–643.
3. *Preining O.* Photophoresis // Aerosol Science. Ed. by C.N. Davies. London: Academic Press, 1966. P. 111–135.
4. *Rohatschek H.* History of photophoresis // History of Aerosol Science / Eds. by O. Preining and E.J. Davis. Wien: Verlag der Österreichischen Akademie der Wissenschaften, 2000.
5. *Schinner A., Rohatschek H.* Stochastic processes associated with photophoresis // J. Aerosol Sci. 2008. V. 39. P. 549–553.
6. *Crookes W.* On (attraction and) repulsion resulting from radiation // Phil. Trans. 1874–1880. V. 164. P. 501–527; V. 165. P. 519–547; V. 166. P. 325–376; V. 168. P. 243–318; V. 170. P. 87–164.
7. *Knudsen M.* Radiometer pressure and coefficient of accommodation // D. Kgl. Danske Vidensk. Selskap, Math.-Fys. Medd. 1930. V. 11, N. 1. P. 1–75.
8. *Rubinowicz A.* Radiometerkräfte und Ehrenhaftsche Photophorese (I and II) // Ann. Phys. 1920. V. 62, N. 4. P. 691–715, 716–737.
9. *Rohatschek H.* Über die Kräfte der reinen Photophorese und der Gravitophotophorese // Acta Physica Austriaca. 1956. V. 10. P. 267–286.
10. *Rohatschek H.* Semi-empirical model of photophoretic forces for the entire range of pressures // J. Aerosol Sci. 1995. V. 26. P. 717–734.
11. *Ehrenhaft F., Reeger E.* Sur la photophorèse transversale // Comptes Rendus Acad. Sci. 1951. V. 232. P. 1922–1924.
12. *Wilflinger E.* Über die Abhängigkeit der Elektrophotophorese von der Lichtintensität und vom Gasdruck // Z. Phys. 1931. V. 71. P. 658–677.
13. *Lustig A., Söllner A.* Über Photophorese von Silberpartikeln // Z. Phys. 1932. V. 79. P. 823–842.
14. *Arnold S., Pluchino A.B., Leung K.M.* Influence of surface-mode-enhanced local fields on photophoresis // Phys. Rev. A. 1984. V. 29. P. 654–660.
15. *Rohatschek H.* The role of gravitophotophoresis for stratospheric and mesospheric particles // J. Atmos. Chem. 1984. V. 1. P. 377–389.
16. *Rohatschek H.* Levitation of stratospheric and mesospheric aerosols by gravito-photophoresis // J. Aerosol Sci. 1996. V. 27. P. 467–475.
17. *Pueschel R.F., Verma S., Rohatschek H., Ferry G.V., Boiadjieva N., Howard S.D., Strawa A.W.* Vertical transport of anthropogenic soot aerosol into the middle atmosphere // J. Geophys. Res. 2000. V. 105. P. 3727–3736.
18. *Cheremisin A.A., Vassilyev Yu.V., Horvath H.* Gravitophotophoresis and aerosol stratification in the atmosphere // J. Aerosol Sci. 2005. V. 36. P. 1277–1299.
19. *Krauss O., Wurm G.* Photophoresis and the pileup of dust in young circumstellar disks // Astrophys. J. 2005. V. 630. P. 1088–1902.
20. *Rohatschek H.* Zur Theorie der Gravitophotophorese // Acta Physica Austriaca. 1956. V. 10. P. 227–238.
21. *Zulehner W., Rohatschek H.* Photophoresis of nonspherical bodies in the free molecular regime // J. Colloid Interface Sci. 1990. V. 138. P. 555–564.
22. *Rohatschek H.* Zur Dynamik der Photophorese // Acta Physica Austriaca. 1969. V. 30. P. 57–82.
23. *Happel J., Brenner H.* Low Reynolds Number Hydrodynamics. N.Y.: Prentice-Hall, Englewood Cliffs, 1965.
24. *Rohatschek H., Zulehner W.* The resistance force on nonspherical particles in the free molecular regime // J. Colloid Interface Sci. 1987. V. 119. P. 378–387.
25. *Rohatschek H.* Direction, magnitude and causes of photophoretic forces // J. Aerosol Sci. 1985. V. 16. P. 29–42.
26. *Tauzin P.* Photophorèse et magnétophotophorèse des particules de fer oméga a différentes pressions // Comptes rendus Acad. Sci. 1950. V. 230. P. 77–79.